Biochimica et Biophysica Acta, 1141 (1993) 95–104

BBABIO 43744

Reactions of the membrane-bound cytochrome *bo* terminal oxidase of *Escherichia coli* with carbon monoxide and oxygen

Barbara Bolgiano [a,1], Ian Salmon [b] and Robert K. Poole [a]

[a] *Microbiology Group, Division of Life Sciences, King's College London, London (UK) and* [b] *Biological Laboratory, University of Kent, Canterbury, Kent (UK)*

(Received 6 April 1992)

Key words: Cytochrome *o*; Quinol oxidase; Carbonyl cytochrome; Oxygen binding; Potentiometry; (*E. coli*)

The cytochrome '*bo*' quinol oxidase of *Escherichia coli* contains 2 mol of haem, one or both of which are 'haem O'. One of the haems forms, with the single copper present, a binuclear site for ligand binding and oxygen reduction. Cytoplasmic membranes from a strain of *E. coli* lacking the alternative cytochrome *bd* quinol oxidase, and having amplified levels of cytochrome *bo*, were used to study oxygen and carbon monoxide reactivity with this oxidase. The high-spin ligand-binding haem was identified from its contribution to the Soret region and the shift in midpoint potential from +211 to +477 mV in the presence of CO. Oxidative titration of a CO-liganded sample was accompanied by a decrease in the contribution from a photodissociable CO-binding haem. The photodissociation spectrum was typical of a high-spin haem. Photolysis of CO-liganded, reduced membranes in the presence of O_2 at sub-zero temperatures revealed O_2 binding and cytochrome oxidation characterized by differential absorbance changes in the α-spectral region. Monitoring by epr spectroscopy of the same reaction sequence at −80°C revealed a slight increase in $g = 6$ signal intensity immediately after photolysis attributable to cytochrome *o* oxidation prior to Cu oxidation. Subsequent decline in the $g = 6$ signal and appearance of a $g = 3$ signal indicated sequential electron flow from low-spin to high-spin haems and copper oxidation, suggesting that a second haem carries electrons from ubiquinol to the binuclear centre.

Introduction

Bacterial cytochrome oxidases represent a functionally and structurally diverse group of electron-transfer proteins [1,2]. Like most bacteria, *Escherichia coli* synthesizes more than one terminal oxidase, each catalyzing the oxidation of ubiquinol by molecular oxygen [3]. One of these, cytochrome *bo*, contains two haems and one copper. The high-spin haem binds CO and, with the copper, forms a binuclear reaction centre [4] where oxygen is bound and reduced [5]. The other haem is low-spin and six-coordinate. All three prosthetic groups are located in subunit I of the oxidase [6]. The nature of the haems and the lack of Cu_A distinguishes this oxidase from mitochondrial and bacterial aa_3-type cytochrome oxidases which, in other respects, it closely resembles [7–9]. Recently, the *E. coli* oxidase has also been shown to pump protons across the cytoplasmic membarne [3,10].

Although the spectral characteristics of the CO compound of cytochrome *o* were clearly established in Chance's photochemical action spectroscopy [11,12] and later photodissociation spectra [5], the contributions of the two haems to reduced minus oxidized difference spectra have remained controversial despite numerous attempts to resolve them, particularly using potentiometric titrations (for surveys of early work, see Refs. 1,2,13). The original suggestion made by Scott and Poole [14] that the ligand-binding cytochrome *o* makes only a small contribution to the α-region of the absorbance of the reduced state has recently received support from spectral studies of the isolated oxidase [3,15]. The absorption characteristics reflect the presence in this oxidase of a novel haem O with a haem A-like structure [15] that gives a pyridine haemochrome spectrum in which the α and β bands in the reduced form are shifted about 4 nm to the blue relative to the corresponding spectrum of haem B (protohaem). The atypical pyridine haemochrome was first reported by us [16] in membranes of a cytochrome *o*-over-producing strain (RG145; [17]), in which detailed potentiometric analyses of the spectral contributions of the oxidase to

Correspondence to: R.K. Poole, Microbiology Group, Division of Life Sciences, King's College London, Campden Hill Road, London W8 7AH, UK.

[1] Present address: Glycoconjugates Section, MRC Clinical Research Centre, Watford Road, Harrow HA1 3UJ, UK.

Abbreviation: SSR, sum of squared residuals.

the α- and Soret regions were also made [16]. It has been suggested [15] that the oxidase complex contains two haems of the O-type, and that preparations of the oxidase contain in addition variable, sub-stoichiometric amounts of cytochrome *b*-556. For clarity, however, and consistent with contemporary work on this oxidase, the complex is described here as cytochrome *bo*. In this paper, we extend previous redox analyses to titrations performed in the presence of CO and exploit the technique of low temperature photodissociation to describe the reactions of cytochrome *o* with CO and O_2 and the subsequent oxidation of cytochrome(s) *b*.

Materials and Methods

Strains and growth conditions

E. coli K-12 strains RG145 and GO103 were provided by R.B. Gennis, University of Illinois, Urbana. Strain GO103 (F^-, *rpsL, thi, gal, Δcyd1*::Km^R) is a mutant deficient in the *d*-type cytochrome oxidase. Strain RG145 (F^-, *rpsL, thi, gal, nadA, lon 100, cyo, srl*::Tn*10 recA56* (Ap^R, Tc^R)) is a cytochrome *o* oxidase over-expressing strain, which also lacks the cytochrome *bd*-terminal oxidase [17]. Cells were grown at 37°C with high aeration on '56' media [18] (pH 7.0), supplemented with a Mo- and NO_3^--free trace elements solution ([19]; 10 ml/l), Luria broth ([20]; 50 ml/l), and glycerol (4 ml/l). After autoclaving, the medium was aseptically supplemented with nicotinic acid and thiamine HCl (each at 0.5 mg/l, final), $MgCl_2$ (1 mM final) and ampicillin (100 μg/ml, final). A 500 ml 18.5 h starter culture, grown in a 2 l flask, was used as inoculum for a 10 l batch growth in a stirred Biostat V 12l fermenter (Braun) sparged with air at 8 l/min. Cells were harvested in the stationary phase of growth (apparent absorbance at 600 nm of 3) after 17–24 h growth, by centrifugation using an Alpha-Laval continuous flow centrifuge and subsequently by centrifugation of the slurry at 12500 × *g* (r_{av} 14.4 cm) for 15 min. Cells were frozen at −20°C until required. Cells typically contained 0.32 nmol cytochrome *o*/mg protein, an approx. 6-fold amplification over levels in wild-type cells.

Cytoplasmic membrane preparation

All procedures were carried out at 4°C. Thawed cells were washed twice with a buffer that contained 0.1 M Tes, 20 mM magnesium acetate, 0.25 M sucrose and 0.25 mM EGTA (pH 7.0) and were resuspended to approx. 1/10 the original volume in the same buffer. To a homogenized suspension was added the proteinase inhibitor phenylmethylsulphonyl fluoride (1 mM final) and a few grains of proteinase-free DNase I. Cells were broken by one passage through a French Pressure cell (Aminco) at 138 MPa and the cell lysate was obtained by centrifugation at 12500 × *g* (r_{av} 10.7 cm) for 20 min. Membrane fragments were then obtained by centrifuging the lysate (low-speed supernatant) at 150000 × *g* (r_{av} 7.35 cm) for 90 min at 4°C. The membrane fraction was suspended in 50 mM Tes, 5 mM EDTA (pH 7.0), homogenized and respun as above. The washed membranes were resuspended in the Tes/EDTA buffer, homogenized and frozen. Membranes contained around 0.52 nmol cytochrome *o*/mg membrane protein.

Potentiometric titrations

Redox titrations were based on [21] as modified by Bolgiano et al. [16]. The buffer (pH 7.0) contained 150 mM Tes, 3 mM EDTA. Titrations in the presence of CO were performed by reducing the sample in the titration cuvette [21] to approx. −150 mV with an anaerobic solution of Na dithionite, then sparging for 5 min with CO through a fine tube, which had been smeared with a trace of antifoam, and could be lifted in and out of the membrane suspension as required. Where redox states were measured at room temperature, CO was blown over the surface of the stirred sample for an additional 40 min before beginning the oxidative titration. For low-temperature experiments, the titration was performed in a fume hood under a slight positive pressure of CO. Samples were removed from the stirred titration chamber into 0.2 cm pathlength cuvettes via a transfer tube that could be lowered into the membrane suspension. The cuvette, which had been previously gassed for a few min with CO, was then immediately frozen in liquid nitrogen. Redox titration data were analyzed by fitting the absorbance values to the Nernst equation [16].

Spectroscopy

Optical difference spectra were recorded using a Johnson Foundation SDB-3 dual-wavelength scanning spectrophotometer [22]. A 4 nm spectral bandwidth was used and the scan rates were as indicated. The reference wavelength was 580 nm. During a redox titration, a fully reduced or fully oxidized scan was usually used as a reference. For CO titrations, the CO + reduced scan was used as baseline.

For low-temperature photodissociation spectra [23], redox-poised samples in liquid N_2 were equilibrated in the dark at −78°C in a solid CO_2/ethanol bath for about 20 min until transfer to the cuvette holder at −60 to −100°C ± 1°C, as indicated in the legends. The sample was scanned twice to obtain a baseline and then photolyzed by 90 s exposure to light from a 150 W projector lamp focused onto one limb of a bifurcated light guide [23]. After photolysis, the sample was immediately scanned using the pre-photolysis spectrum as baseline.

EPR spectra were obtained using a Bruker ER200D spectrometer (Bruker Analytische Tesstechnik, Silber-

streifen, D-7512 Rheinstetten H, Germany) equipped with a variable temperature cryostat and liquid helium transfer line (Oxford Instruments, Osney Mead, Oxford, UK).

Sample preparation for low temperature ligand exchange

For ligand-exchange experiments, the method of Chance et al. [24] was followed with the following modifications. Samples were prepared in 1 ml capacity (0.2 cm path length) Perspex cuvettes. Membranes were diluted (approx. final conc. 10 mg/ml for optical spectra, 20 mg/ml for EPR spectra) in a buffer that contained 25 mM Tes, 2.5 mM EDTA (pH 7.0); ethylene glycol (30% v/v) and sodium succinate (pH 7) (20 mM, final) were added. The sample was incubated at room temperature for 30 min to allow reduction of the

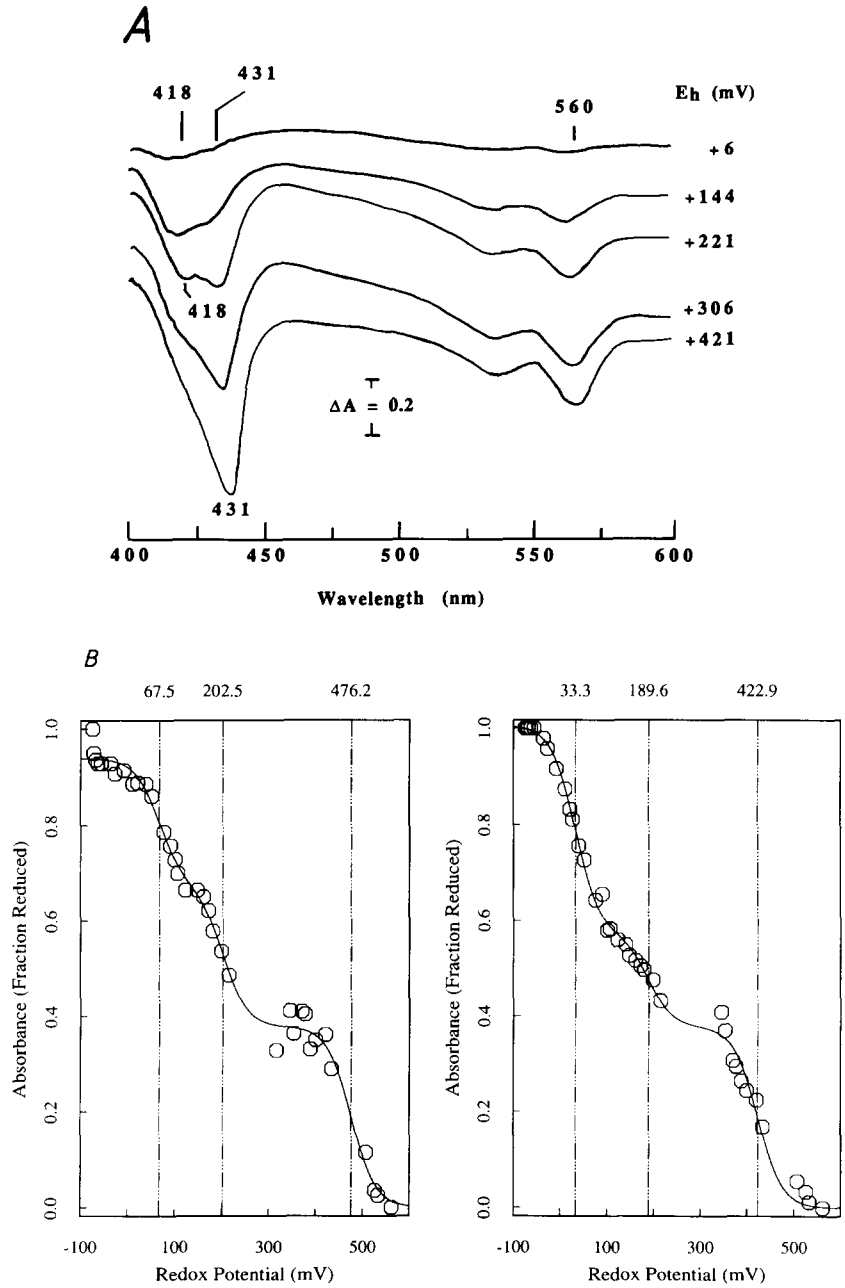

Fig. 1. Potentiometric analysis of *E. coli* RG145 membranes at 25°C in the presence of carbon monoxide. (A) Difference spectra were recorded over the range 400 nm to 600 nm with 575 nm as reference wavelength. Spectra shown are of samples poised at +6, +144, +221, +306 and +421 mV during an oxidative titration with ammonium persulfate. The spectrum of the reduced sample bubbled with CO (poised at −117 mV) is the subtracted baseline. (B) Plots of redox potentials versus absorbance at 455 minus 432 nm (left), and 580 nm minus 560 nm (right). Lines drawn represent the best fit analyses for three components (SSR = 0.018 (left) and 0.013 (right)). Membrane protein concentration was 15 mg/ml.

oxidase and then bubbled with CO for 3–4 min. All subsequent procedures were carried out in dim light. Cuvettes were cooled in a solid CO_2/ethanol bath at −25°C for 5 min. Where indicated, O_2 was added by stirring the sample with a coiled stainless steel wire (2/s) for 30 s to give about 360 μM O_2 [24]. Immediately, the cuvette was placed in a −78°C dry ice/ethanol bath and stored for at least 5 min. Samples (0.5 ml total) were prepared in EPR tubes in a similar manner using appropriate stirrers and bubbling tubing. After equilibration at −78°C, cuvettes were transferred to the sample compartment of the dual-wavelength spectrophotometer. Temperature control (±1°C) was achieved by blowing a stream of N_2, cooled by circulation through a copper coil immersed in liquid N_2, over the base of the cuvette [23]. Photolysis was performed as described above and samples scanned at indicated times following photolysis.

Analytical methods

Protein was determined according to a modified Lowry method [25] using bovine serum albumin as a standard. The following extinction coefficients for the calculation of cytochromes *b* and *o* at room temperature were used [26]: $\epsilon_{414-430\,nm} = 145\ cm^{-1}\ mM^{-1}$ for cytochrome *o* from CO difference (CO + reduced minus reduced) spectra and $\epsilon_{560-580\,nm} = 18.7\ cm^{-1}\ mM^{-1}$ for cytochrome *b* from fully reduced minus fully oxidized spectra. The former value is probably too low [16] perhaps by as much as 2-fold [15].

Ubiquinol oxidase assays [27] were performed spectrophotometrically following the oxidation of ubiquinol-1 (gift of Hoffman LaRoche) in 60 mM Tris-HCl (pH 7.5). An ethanolic solution of ubiquinol was reduced by adding μl aliquots of an acidified solution of sodium borohydride (5 mg/ml) until almost colourless. To a quartz cuvette, 10 μl of ubiquinol solution was added to buffer (2.5 ml final), and the reaction was started by adding 10–50 μl of a membrane suspension. The absorbance increase at 275 nm accompanying ubiquinol oxidation was followed to completion at 25°C. A few crystals of ammonium persulphate were added to confirm the endpoint. An extinction coefficient for ubiquinone of $\epsilon_{275} = 12.25\ mM^{-1}\ cm^{-1}$ was used [28].

Chemicals

General reagents were from Fisons or BDH and were of AnalaR grade wherever possible. 1,2-Naphthoquinone was from ICN Pharmaceuticals (Plainview, New York), 1,2-naphthoquinone-4-sulphonic acid was from Koch-Light, and 2,3,5,6-tetramethyl phenylenediamine was from Aldrich. Bovine serum albumin, Tes, PMSF, proteinase-free DNase I, 2-hydroxy-1,4-naphthoquinone, benzyl viologen, and phenazine methosulfate were from Sigma. Argon, oxygen-free nitrogen and CO were from BOC Special Gases.

Results and Discussion

Ubiquinol oxidase activity

The ubiquinol oxidase specific activities in both the over-expressing strain (RG145) and in the cytochrome *bd*-deficient strain (GO103) were similar with turnover numbers (μM ubiquinol oxidized/s per μM cytochrome *o*) of 300 s^{-1} and 341 s^{-1}, respectively. The reaction was found to be first order with respect to ubiquinol concentration in both cases (data not shown). Thus, the RG145 membranes used in this paper allowed spectral analysis of the amplified cytochrome *bo* complex, without interference from the alternative oxidase, cytochrome *bd*, and without recourse to purification of the oxidase, which may result in alteration of redox potentials and loss of cytochrome(s) *b* involved in electron transfer from ubiquinone [15].

Potentiometric titrations in the presence of CO

Previous potentiometric analyses of membranes from an *E. coli* strain containing amplified levels of the cytochrome *bo* terminal oxidase were performed in the absence of CO [16] and revealed three potentiometrically distinct contributions to the Soret band and two to the α-band. Early [14] and recent [15] evidence shows that the ligand-binding cytochrome makes only a small, broad contribution to the α-band, suggesting that the Soret region should provide less equivocal data on the *b* and *o* type cytochromes. CO binds at the O_2-binding haem in its Fe(II) state, forming, in the absence of O_2, a stable adduct and raising the redox potential of the bound haem. Thus, using membranes from strain RG145, reduced and bubbled with CO in an anaerobic cuvette, we recorded absorption spectra in the Soret and α-regions during an oxidative titration with ammonium persulphate.

Spectra in Fig. 1A are presented as difference spectra with the reduced, CO-liganded sample, poised at −117 mV, as reference. During the course of the titration, troughs appeared at 418, 431, 530 and 560 nm. The 418 nm trough was attributed to loss of the CO-liganded form, whereas troughs at about 431, 530 and 560 nm were attributed to oxidation of low-spin *b*- or *o*-type cytochromes. In the early stages of titration, the 418 nm trough dominated the Soret region but the maximum intensity of the trough later shifted to 431 nm; the α- and β-bands developed throughout. Fig. 1B plots the changes at 432 and 560 nm relative to appropriate reference wavelengths as a function of ambient potential. The data for the absorbance changes at 455–418 nm were not well fitted by the Nernst equation (not shown), two $n = 1$ components of $E_{m7} + 61$ mV and 213 mV giving sum of squared residuals (SSR) = 0.11. The adjacent 431 nm trough, however, titrated with E_{m7} values of +67.5 mV (26%), +202.5 mV (30%) and +476.2 mV (38%); the fit for three $n = 1$

TABLE I

Analyses of potentiometric titrations of the Soret and α-regions in the absence and presence of CO

The best-fitting parameters for the areas under absorbance peaks in the absence of CO are from Ref. 15. Values from oxidative titrations in the presence of CO are from Fig. 1. Values given are E_{m7} (mV) and relative amount (in parentheses). Arrows indicate midpoint potential shifts elicited by CO.

Soret region		α-region	
−CO	+CO	−CO	+CO
−97 (0.22)			
+55 (0.48) →	+68 (0.26)	+57 (0.59) →	+33 (0.44)
+211 (0.22) →	+202 (0.3)	+227 (0.45) [a] →	+190 (0.19)
↘	+477 (0.38)	↘	+423 (0.38)
+408 (0.14)			

[a] broad signal, 556 to 565 nm.

components was good (SSR = 0.018). These values were close to those observed at 560 nm with E_{m7} values of +33.3 mV (44%), +189.6 mV (19%) and +422.9 mV (38%), with SSR = 0.013.

Table I compares titrations in the absence and presence of CO for both Soret and α regions. As proposed previously [16], in the absence of CO, the major Soret contribution (E_{m7}, +55 mV) probably corresponds to the component titrating at around +57 mV in the α-region. During titration with persulphate, the presence of CO increased the apparent mid-point potential of the former by 13 mV and decreased the latter by 24 mV. These shifts in the mid-point of the low potential component suggest little binding of CO, and were much smaller than those reported by Withers and Bragg [29] who described CO-induced shifts from −58 to −92 mV and from +127 to +51 mV during oxidative titrations with ferricyanide of the purified oxidase complex. Their results were interpreted as reflecting sensitivity of a low potential haem to modification by ferricyanide. The simplest interpretation of the present data is that a major contributor to the +211 mV (Soret) band is the ligand-binding cytochrome *o* whose mid-point potential is raised to +477 mV in the presence of CO. Similar conclusions were drawn previously [29]. The corresponding band in the α region had its mid-point raised from +227 to +423 mV; it is notable that the +227 mV component has a broad α-absorbance [16], consistent with the view [15] that its contribution to the α-region is small.

Photodissociability during redox titrations in the presence of CO

In an attempt to confirm the contribution of the CO-binding haem to potentiometric titrations, redox-poised samples from an oxidative titration in the presence of CO were frozen and used for photodissociation spectroscopy. The characteristic photodissociation spectrum of cytochrome *o*, peak at 430 nm and a trough at 414 nm [5], is detectable only when CO

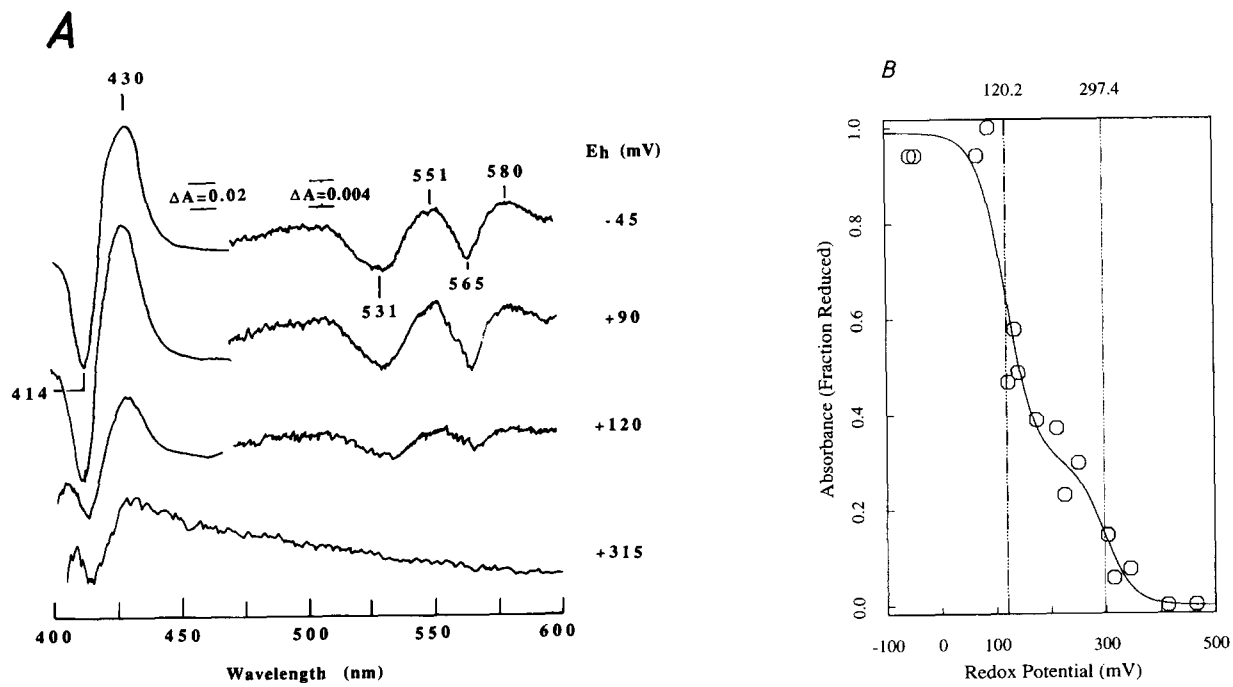

Fig. 2. The effect of redox potential on photodissociation of *E. coli* cytochrome *o* at −100°C. (A) Photodissociation spectra were taken of samples poised at the solution potentials shown after 90 s exposure to white light, with the pre-photolysis spectrum as subtracted baseline. Spectra were scanned with 580 nm as reference wavelength, at 1.43 nm/s. Spectra were recorded in cuvettes with a pathlength of 0.2 cm. (B) Best-fitting Nernst curve of $A_{430-414\,nm}$ versus redox potential (E_h). Membranes were suspended at 9.6 mg/ml.

remains bound to the reduced haem in samples withdrawn from the titration cuvette; thus, spectra recorded after exposure to light indicate the amount of photolysable haem-CO complex in the samples. The spectra in Fig. 2A are post-photolysis minus pre-photolysis photodissociation spectra recorded at −100°C. Fig. 2B shows results pooled from a number of such titrations. At progressively higher potentials, the absorbance difference at 430 minus 414 nm declined as predicted. Most of the total charge occurred between +90 and +130 mV, with E_{m7} = 120.2 mV (n = 1; 68.9% of the total signal). At higher potentials, a more gradual decrease in the level of the photosensitive CO compound occurred with an apparent mid-point of +297.4 mV (n = 1; 30.1% of the total). The SSR was 0.075. An alternative analysis (not shown) of the data treated the titration as being monophasic and gave an E_{m7} of +154 mV (n = 1), but the fit was poor (SSR = 0.314). The probability that the data were not the same as the one-component model is 0.96.

In assigning cytochrome *o* to one of these phases, there are a number of points to consider. Previous studies have shown that the half-time for CO reassociation with the Fe(II) haem is about 20 min at −92°C [5], so that the concentration of cytochrome *o* is unlikely to be underestimated by rapid combination of CO following exposure to actinic light. However, the experimental design might underestimate the assay of the photodissociable CO-cytochrome *o* complex on two counts. First, detection of the unliganded cytochrome *o* after photolysis relies on relatively slow recombination of the dissociated CO. There is good evidence that the 'fast' recombination (i.e., complete at −100°C within the time taken for conventional wavelength scanning) observed for many protohaem proteins (i.e., myoglobin) and for cytochrome *d* [30] in the *E. coli bd* terminal oxidase is due to the absence of copper and CO recombination directly to the haem. However, in the case of cytochromes a_3 and *o*, the copper atom 'traps' the dissociated CO, which returns only slowly to haem a_3 or *o* in a photo-independent fashion. This view is supported by infrared observation of a Cu-CO band in mitochondrial cytochrome aa_3 [31,32], *Thermus thermophilus* cytochrome aa_3 [33] and *E. coli* cytochrome *o* [34]. Furthermore, copper depletion of the cytochrome *bo* complex in *E. coli* by copper-limited chemostat growth causes gross underestimation of the amount of cytochrome *o* when assayed by photodissociation spectroscopy [35], due to rapid recombination of CO. In the experiment of Fig. 2B, Cu(I) oxidation (E_m ~ 370 mV;[4]), as high potentials are approached, would allow rapid recombination to the unliganded cytochrome *o*, underestimating the amount detectable on photolysis and tending to raise the apparent E_m.

Second, the low spin, low potential cytochrome *b* component of the complex, which does not bind CO, would be oxidized early in the oxidative titration; electron re-distribution following photolysis might also underestimate photogeneration of the undissociated cytochrome *o*. Finally, a change in the geometry of the Fe-CO bond with respect to the haem plane, due to solvent interaction or amino acid changes in the ligand-binding pocket, are likely to affect photodissociation [36]. With these caveats, and given the difficulty of obtaining numerous data points in this type of experiment, we assign the higher potential phase of the titration in Fig. 2b to the CO-binding cytochrome *o*.

Low temperature ligand exchange reactions

The reactions of cytochrome *o* with carbon monoxide or with oxygen and subsequent electron transfer following photolysis of the CO-liganded oxidase at sub-zero temperatures have previously been reported only with intact cells [5]. Membranes from the cytochrome *o* over-producing strain were reduced with succinate, bubbled with CO, then frozen at −78°C before transfer to the temperature-equilibrated sample compartment of the dual-wavelength spectrophotometer. Photolysis at −100°C in the absence of oxygen gave a difference spectrum (with the prephotolysis spectrum as reference) that showed troughs at 415, 535 and 566 nm attributed to loss of the CO-liganded form (Fig. 3). The band positions were similar to the absorption maxima reported [12] in photochemical action spectra and in the conventional CO difference spectrum of the isolated oxidase [15]. Further, as reported in Ref. 15, there was no significant band (i.e., peak in Fig. 3; trough in their Fig. 1) that could be attributed

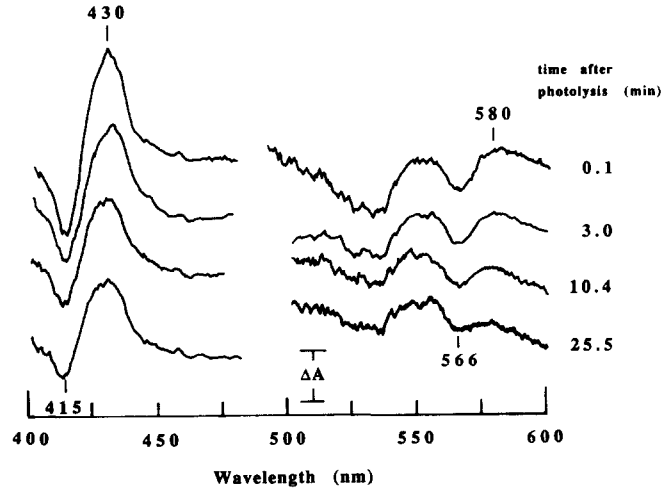

Fig. 3. Reaction of cytochrome *o* with carbon monoxide at −100°C. Repetitive scans of dithionite-reduced membranes photolyzed in the absence of oxygen are shown with a baseline (reduced +CO) subtracted. The reference wavelength was 580 nm, scan rate 1.43 nm/s, and protein concentration 11 mg/ml. The absorbance bar represents 0.04 A for the Soret and 0.008 A for the α region.

to the α-band of the reduced form, as can the 430 nm peak in Fig. 3.

Continued spectral scanning at -100°C after photolysis revealed recombination of CO, as the symmetrical approach towards the baseline (representing the liganded form) of the 415 and 430 nm signals [5]. At 15 min (not shown), the Soret absorbance difference had decayed by about 50% and the rebinding was sensitive to further photolysis, restoring the original photodissociation spectrum (results not shown). Photosensitivity is generally taken to indicate binding of CO rather than O_2 [37]. The changes in the α region were similar but of lower magnitude. The ratio of the peak-trough amplitude in the Soret region (430–415 nm) to that in the a region (566–550 nm) was about 29. This compares with a value of 32 for myoglobin and higher values for several high spin b-type haem proteins [38] and with a value, measured from the CO difference spectrum in [15], at the above wavelength pairs, of 24.

The above experiment was modified by aerating the CO-treated, succinate-reduced sample at -25°C before freeze-trapping. Under these conditions, in the dark, the O_2 introduced does not displace CO from the carbonmonoxy compound, allowing activation of the reaction between the oxidase and O_2 in the frozen state after photolysis of the CO adduct [5,24]. At -80°C, the first difference spectrum (using the prephotolysis, CO-liganded state as reference) showed a trough at 415 nm and a split trough at 554/562 nm (Fig. 4). At this temperature, the 430 nm peak of the unliganded cytochrome *o* had decayed within the time taken to complete the first scan. This results from O_2 binding; in the absence of O_2 at these temperatures, the 430 nm band decays only slowly, whether the experimental material is intact cells (above, [5]) or membranes (R.K. Poole and I. Salmon, unpublished data). The α region in Fig. 4 was also quite distinct from that observed in the absence of oxygen (Fig. 3) the 565 nm trough having been replaced by a prominent band centred at about 572 nm and a split trough with 562 nm as the dominant absorbance difference. Repetitive scanning of the photolysed sample revealed intensification of the trough at 428 nm and differential development of the troughs at 554 and 562 nm, all attributable to oxidation of *b*-type cytochrome(s). The later oxidation of the *b*-type cytochrome at 554 nm is consistent with the lower mid-point potential of the short wavelength component [16]. The fully oxidized minus reduced + CO difference spectrum (Fig. 4, bottom) had features similar to that of the sample 30 min after photolysis. The sample appeared to be only 25% oxidized at this point. This can be attributed to incomplete occupancy of the CO adduct, partial photolysis, and/or formation of uncharacterized intermediates. For example, in comparison with cytochrome aa_3, haem *a* is thought to be only partially oxidized (approx. 40%)

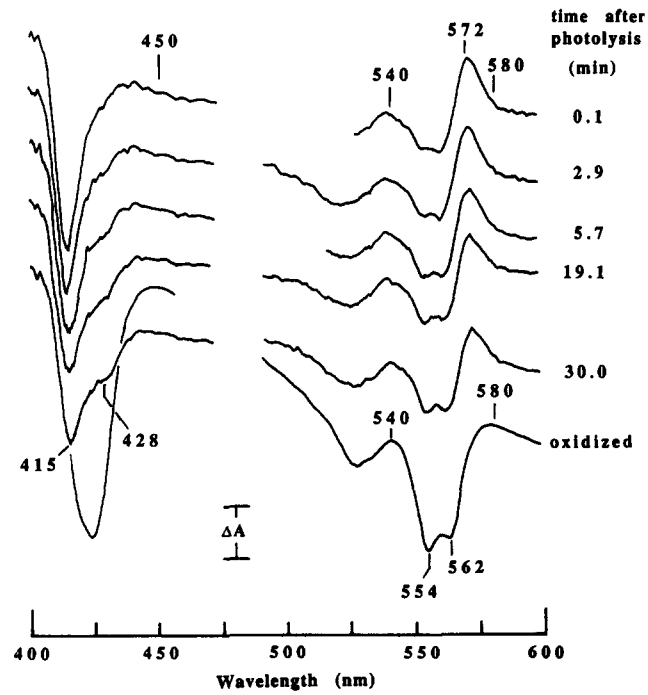

Fig. 4. Reaction of cytochrome *bo* with oxygen after photolysis of the carbonmonoxy compound in membrane suspensions at -80°C. The spectrum of the pre-photolysis (CO + reduced) sample was used as subtracted baseline. The absorbance bar represents for the timed scans, 0.04 A (Soret) and 0.2 A (α region) and for the fully oxidized sample, 0.08A (Soret) and 0.04A (α region). Reference wavelength was 580 nm, scan rate 1.43 nm/s and protein concentration 11 mg/ml.

in intermediates II and III [39] with full reduction occurring only on electron transfer from cytochrome *c* at temperatures above -60°C [40].

The absorbance changes in the difference spectra of Fig. 4 are plotted in Fig. 5. The increasing depth of the cytochrome *b* troughs (562, 554 and 428 nm) are shown as increases in ΔA after photolysis of the carbonmonoxy compound. A Guggenheim analysis [41] gave a good fit (not shown) to first-order kinetics and an apparent rate constant of 0.06 min^{-1} ($t_{1/2} = 11.5$ min). First order kinetics were also observed at -60°C and -70°C (results not shown). At 38 min after the initial photolysis, a second exposure to the actinic light was given, causing further increases in absorbance at 428, 554 and 562 nm. In contrast, the diminishing trough depth at 415 nm was reversed by the second exposure to actinic light. Such light-reversibility is generally taken [37] as demonstrating combination of an oxidase with CO rather than with O_2. Uno et al. [42] have reported two CO binding sites in this oxidase with different sensitivities to photolysis, suggesting that some CO recombination with the oxidase might accompany cytochrome oxidation.

The absorbance changes following photolysis are more easily visualised if the scan obtained 30 min later (part-oxidized) is subtracted from the scan started im-

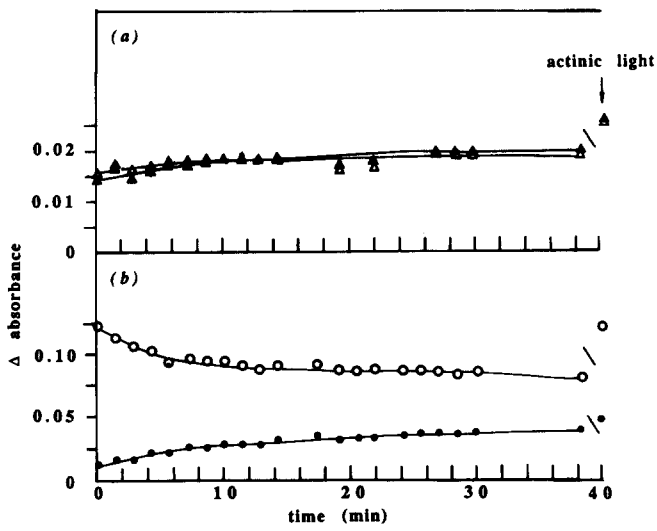

Fig. 5. Plots of absorbance versus time after photolysis of the carbonmonoxy compound of cytochrome *o* shown in Fig. 4. Absorbance values at the following wavelength pairs are shown: (a) 540–562 nm (△), 540–554 nm (▲); (b) 450–415 nm (○); 450–428 nm (●). At 38 min following the first 90 s exposure to active light, samples were again irradiated with actinic light (arrow).

mediately (0.1 min) after switching off the actinic light (Fig. 6a). The difference spectrum showed a prominent peak at 430 nm suggesting that *b*-type cytochrome was oxidized in the 0.1 to 30 min interval. Similarly, the 415 nm trough showed that this component further decreased with time (i.e., approached the baseline) as

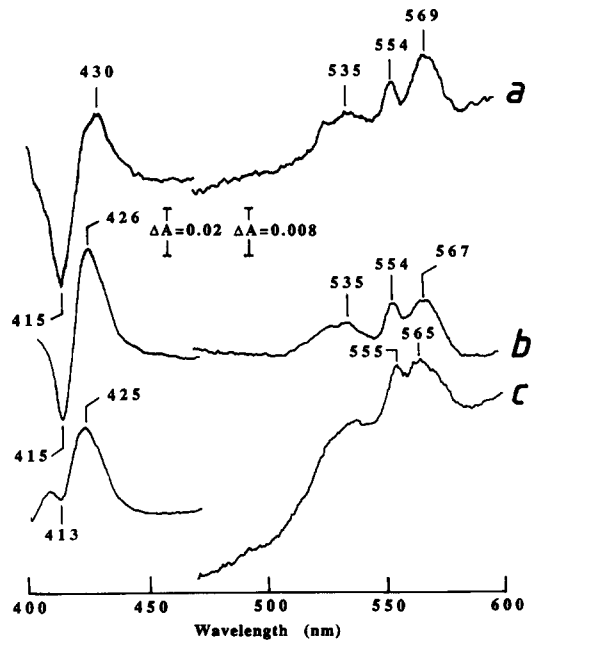

Fig. 6. Difference spectra following photolysis in the presence of oxygen. Scan (a) shows the difference spectrum of the scan taken at 0.1 min in Fig. 4 minus the scan taken after 30 min (part-oxidized sample) at −80°C. Conditions are as described in Fig. 4. Scans (b) and (c) are similar difference spectra from experiments performed at −70°C and −60°C, respectively.

shown in Fig. 5. The α and β regions are of special interest. The 569 nm band (572 nm in the difference spectrum of Fig. 4) was at too long a wavelength to be attributable to the reduced form of any *b*-type cytochrome described in *E. coli*. Since the signal was at its most intense immediately after photolysis, it is unlikely to arise from the CO adduct which it closely resembled in band position. Since the O_2 and CO complexes of myoglobin, for example, [38] are similar, as are the O_2 and CO forms of cytochrome a_3 [43], we tentatively attribute the 569 nm band to the difference spectrum (with a part-reduced form as reference) of the oxy-form of cytochrome *o*, which then decays during the 0.1 to 30 min interval. The broadness of the peak suggests that the band may have contributions from other reduced *b*-type cytochrome(s) near 562 nm. The 554 nm peak was weak but well-resolved and presumably reflected net oxidation of a cytochrome, with an absorption maximum near this wavelength, during the 30 min of observation. The very broad 535 nm band may also have contained contributions from the putative oxy form. Similar difference spectra (i.e., first after photolysis minus last at 30 min) observed at −70°C (Fig. 6b) and −60°C (Fig. 6c) were similar but for the gradual shift of the a peak to 567 then 565 nm, and increase in the 554 nm band. The absence of a 415 nm trough in Fig. 6c indicates that any CO recombination was complete within the first scan after photolysis.

It is striking that the 569 nm absorbance was very intense relative to the Soret band. Using wavelength pairs of 430–450 nm and 569–583 nm, respectively, the Soret/α ratio measurement from Fig. 6 was 3.1. This compares with 11.8 for the reduced (TMPD plus ascorbate) minus oxidized spectrum of the isolated cytochrome *bo* complex [15], and similar values reported by others [26,44], but is close to the ratio (2.8) observed for absolute spectra of cytochrome *a* [45]. Examination of spectra such as those in Fig. 4 recorded within the first 3 min after photolysis predicts that the oxy form, equivalent to compound A of cytochrome a_3 [43] would have a low absorption coefficient relative to the CO form. Thus, the 415 nm trough due to dissociation of CO from reduced cytochrome persisted during cytochrome *b* oxidation indicating that the oxy form has a much weaker absorption than the carbonmonoxy form at this wavelength. Furthermore, if the oxy species were spectrally very similar to the reduced form (430 nm), photodissociation of CO would be followed by little change at 430 nm; in fact, the 430 nm peak decayed prior to extensive cytochrome *b* oxidation. We conclude that the oxy-form of cytochrome *o* resembles the CO form more closely than it does the reduced form in the Soret region and has a prominent a band near 570 nm relative to the oxidized form. The possibility that a mixed population of oxidase intermediates will be present, however, during the reaction sequence

following photolysis as in cytochrome aa_3 [46] allows other interpretations.

EPR studies of the reaction with oxygen

The potentiometric behaviour of the high spin and low spin haems in the cytochrome *bo* complex has recently been studied by EPR in this strain [4]. The high spin signal, which we attribute to the haem of cytochrome *o* titrated as a bell-shaped curve. Mid-points of +180 and +280 mV on the low potential side were attributed to the cytochrome(s), whereas the high potential side was monophasic and the E_{m7} of +370 mV was attributed to Cu. In its Cu(II) state, the Cu is thought to be coupled to cytochrome *o* resulting in a net even spin and EPR undetectability. A low spin haem signal was attributed to cytochrome *b* [4]. In the experiment shown in Fig. 7, membranes in EPR tubes were reduced with succinate, bubbled with CO, and oxygenated at low temperature by stirring with a coiled wire before rapid freezing. Photolysis was performed at −80°C and the samples were trapped at 77 K at the time intervals shown. The magnitude of the high-spin signal at $g = 6$ increased slightly between 0.1 and 1.2 min and then steadily decreased through the rest of the experiment. Even at 1.2 min, the signal was only 25% of the intensity seen in persulphate-oxidized samples. This is probably due to the difficulties of obtaining high occupancy of CO in EPR tubes and of introducing oxygen in a controlled fashion to prevent CO displacement and oxidation prior to photolysis. The small increase in the $g = 6$ signal probably reflected cytochrome *o* oxidation prior to that of Cu(I) which, when oxidised, would have caused a diminution of the $g = 6$ signal through spin-coupling. The low-spin signal ($g = 3$) was not evident until 30 min after photolysis, when it achieved 40% of its maximum intensity. Unequivocal assignment of the signal intensity changes is problematic given that redox changes in the copper and cytochrome *o* each influence the $g = 6$ signal height and that a mixed population of intermediates probably existed over the time period studied. The optical experiments (Fig. 4), however, suggested that oxidation of cytochromes (principally cytochrome *o*) began within 3 min after photolysis. The gradual decrease in the intensity of the $g = 6$ signal, therefore, might reflect gradual reduction of cytochrome *o* by electron transfer from the low-spin cytochrome *b*, while the copper is part-reduced, as well as copper oxidation. The initial rise in the $g = 6$ signal is presumably a result of some electron transfer from reduced cytochrome *o* to oxygen, the oxy-form (being EPR-silent) having formed prior to the recording of optical (Fig. 4) or EPR spectra.

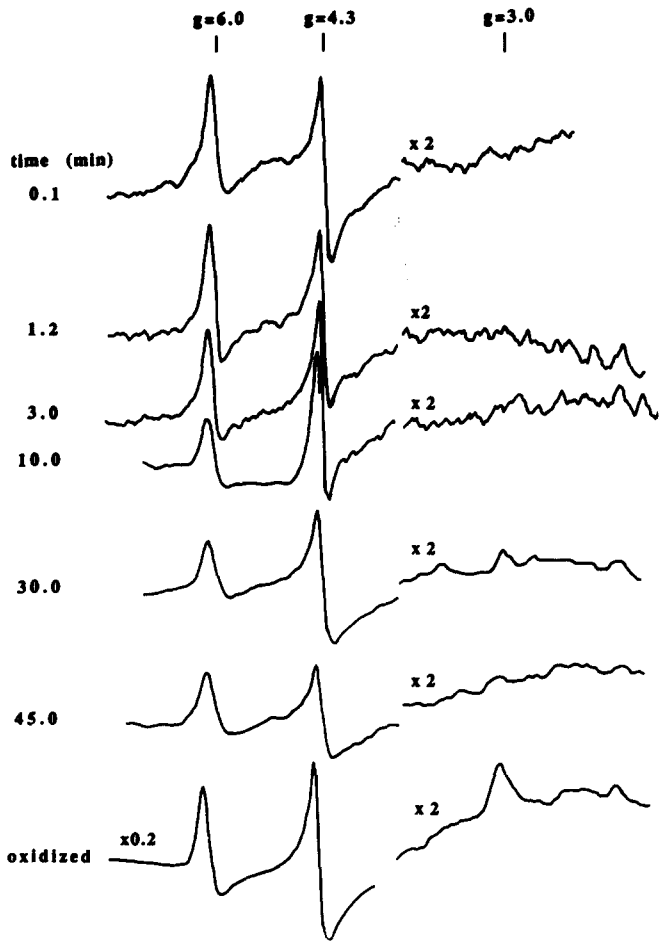

Fig. 7. Development of EPR signals at $g = 6$ and $g = 3$ following photolysis of a CO-treated and reduced sample to which 0_2 had been added at −25°C. Spectra show samples trapped in liquid nitrogen at the indicated times following photolysis at −80°C. The bottom scan is of a sample oxidized by adding a few grains of ammonium persulphate. EPR operating conditions were: temperature, 15 K; microwave frequency, 9.46 GHz; microwave power, 10 mW; field modulation amplitude, 1.25 mT; instrument gain, $5 \cdot 10^5$; time constant, 0.5 s.

Conclusions

Potentiometric redox titrations in the presence of CO have allowed us to determine the contributions to optical spectra of cytochrome *o*, the ligand-binding haem O in the 'cytochrome *bo*' terminal oxidase. We assign a dominant signal in the Soret region and a broad α-band to this haem, having an $E_{m7.0}$ between +211 and +227 mV. The Soret/α ratio in photodissociation spectra is 29, indicative of a high-spin state. Following reaction with oxygen, oxidation of a cytochrome *b* (or perhaps a second haem *o*) with lower $E_{m7.0}$ and absorbing at shorter wavelengths in the a region is observed at low temperatures. EPR spectroscopy of samples trapped at time intervals, after photolysis of the carbonmonoxy compound in the presence of oxygen, reveal oxidation of the respiratory chain components in the order, cytochrome *o*, Cu, cytochrome(s) *b*/*o*. These oxidations are preceded by the formation of an 'oxy' species of cytochrome *o*,

which resembles the CO form in the Soret region but appears to have an additional distinctive absorbance near 570 nm relative to the oxidized form. Further characterization of this form, and an explanation of the apparent photolability of the oxygen adduct, or of super-stoichiometric binding of CO to the oxidase complex, will require further study.

Acknowledgements

We thank Prof. R.B. Gennis for providing the *E. coli* strains used in this work, Alex Houston for assistance in obtaining the EPR spectra and Dr. W.J. Ingledew for discussion and comment. This work was supported by grant GR/E 3496.4 from the UK Science and Engineering Research Council to R.K. Poole and W.J. Ingledew. R.K. Poole thanks the Royal Society and Smith-Kline Foundation for equipment grants.

References

1 Poole, R.K. (1983) Biochim. Biophys. Acta 726, 205–243.
2 Poole, R.K. (1988) In Bacterial Energy Transduction (Anthony, C., ed.), pp. 231–291, Academic Press, London.
3 Puustinen, A., Finel, M., Haltia, T., Gennis, R.B. and Wikstrom, M. (1991) Biochemistry 30, 3936–3942.
4 Salerno, J.C., Bolgiano, B., Poole, R.K., Gennis, R.B. and Ingledew, W.J. (1990) J. Biol. Chem. 265, 4364–4368.
5 Poole, R.K., Waring, A.J. and Chance, B. (1979) Biochem. J. 184, 379–389.
6 Lemieux, L.J., Calhoun, M.W., Thomas, J.W., Ingledew, W.J. and Gennis, R.B. (1992) J. Biol. Chem. 267, 2105–2113.
7 Ingledew, W.J. and Bacon, M. (1991) Biochem. Soc. Trans. 19, 613–616.
8 Saraste, M., Raitio, M., Jalli, T., Chepuri, V., Lemieux, C. and Gennis, R.B. (1988) Ann. N.Y. Acad. Sci. 550, 314–324.
9 Chepuri, V., Lemieux, L., Au, D.C.-T. and Gennis, R.B. (1990) J. Biol. Chem. 265, 11185–11192.
10 Puustinen, A., Finel, M., Virkki, M. and Wikstrom, M. (1989) FEBS Lett. 249, 163–167.
11 Chance, B., Smith, L. and Castor, L. (1953) Biochim. Biophys. Acta 12, 289–298.
12 Castor, L.N. and Chance, B. (1959) J. Biol. Chem. 234, 1587–1592.
13 Poole, R.K. and Ingledew, W.J. (1987) in *Escherichia coli* and *Salmonella typhimurium* Cellular and Molecular Biology (Neidhardt, F.C., Ingraham, J.L., Low, K.B., Magasanik, B., Schaechter M. and Umbarger H.E., eds.), pp. 170–200, American Society for Microbiology, Washington.
14 Scott, R.I. and Poole, R.K. (1982) J. Gen. Microbiol. 128, 1685–1696.
15 Puustinen, A. and Wikstrom, M. (1991) Proc. Natl. Acad. Sci. USA 88, 6122–6126.
16 Bolgiano, B., Salmon, I. Ingledew, W.J. and Poole, R.K. (1991) Biochem. J. 274, 723–730.
17 Au, D.C.-T. and Gennis, R.B. (1987) J. Bacteriol. 169, 3237–3242.
18 Gibson, F., Cox, G.B., Downie, J.A. and Radik, J. (1977) Biochem. J. 164, 193–198.
19 Pirt, S.J. (1967) J. Gen. Microbiol. 47, 181–197.
20 Miller, J. (1972) Experiments in Molecular Genetics, p. 440, Cold Spring Harbor Laboratory, Cold Spring Harbor.
21 Dutton, P.L. (1978) Methods Enzymol. 54, 411–435.
22 Williams, H.D. and Poole, R.K. (1987) J. Gen. Microbiol. 133, 2461–2472.
23 Jones, C.W. and Poole, R.K. (1985) Methods Microbiol. 18, 285–328.
24 Chance, B., Graham, N. and Legallais, V. (1975) Anal. Biochem. 67, 552–579.
25 Markwell, M.A.K., Haas, S.M., Bieber, L.L. and Tolbert, N.E. (1978) Anal. Biochem. 87, 206–210.
26 Kita, K., Konishi, K. and Anraku, Y. (1984) J. Biol. Chem. 259, 3368–3374.
27 Kita, K., Konishi, K. and Anraku, Y. (1986) Methods Enzymol. 126, 94–113.
28 Redfearn, E.R. (1967) Methods Enzymol. 10, 381–384.
29 Withers, H.K. and Bragg, P.D. (1990) Biochem. Cell Biol. 68, 83–90.
30 Poole, R.K., Sivaram, A., Salmon, I. and Chance, B. (1982) FEBS Lett. 141, 237–241
31 Fiamingo, F.G., Altschuld, R.A., Moh, P.P. and Alben, J.O. (1982) J. Biol. Chem. 257, 1639–1650.
32 Alben, J.O., Moh, P.P., Fiamingo, F.G. and Altschuld, R.A. (1981) Proc. Natl. Acad. Sci. USA 78, 234–237.
33 Einarsdóttir, O., Killough, P.M., Fee, J.A. and Woodruff, W.H. (1989) J. Biol. Chem. 264, 2405–2408.
34 Chepuri, V., Lemieux, L., Hill, J., Alben, J.O. and Gennis, R.B. (1990) Biochim. Biophys. Acta 1018, 124–127.
35 Ciccognani, D.T., Hughes, M.N. and Poole, R.K. (1992) FEMS Microbiol. Lett. 94, 1–6.
36 Orii, Y. (1978) Advances in Biophysics (Kotani, M. ed.), Vol 11, pp. 285–308, University Park Press, Baltimore.
37 Thompson, A.J. (1977) Nature 265, 15–16
38 Wood, P.M. (1984) Biochim. Biophys. Acta 768, 293–317.
39 Clore, G.M., Andreasson, L.-E., Karlsson, B., Aasa, R. and Malmstrom, B.G. (1980) Biochem. J. 185, 139–154.
40 Chance, B., Saronio, C., Leigh, J.S. Jr., Ingledew, W.J. and King, T.E. (1978) Biochem. J. 171, 787–798.
41 Gutfreund, H. (1972) Enzymes: Physical Principles, p. 118, Wiley and Sons, London.
42 Uno, T., Nishimura, Y., Tsuboi, M., Kita, K. and Anraku, Y. (1985) J. Biol. Chem. 260, 6755–6760.
43 Chance, B., Saronio, C. and Leigh, J.S. (1975) J. Biol. Chem. 250, 9226–9237.
44 Matsushita, K., Patel, L. and Kabak, H.R. (1984) Biochemistry 23, 4703–4714.
45 Vanneste, W.H. (1966) Biochemistry 5, 838–848.
46 Han, S., Ching, Y.-C. and Rousseau, D.L. (1990) Proc. Natl. Acad. Sci. USA 87, 2491–2495.